AGU PUBLICATIONS

Geophysical Research Letters

RESEARCH LETTER
10.1002/2014GL060551

Key Points:
- Extreme swings of the SPCZ occur with El Niño eastern Pacific warming
- Extreme El Niño is not required to induce an extreme swing of the SPCZ
- Extreme swings occur more often with EP-type El Niño under greenhouse warming

Supporting Information:
- Readme
- Tables S1–S4 and Figures S1–S4

Correspondence to:
S. Borlace,
simon.borlace@csiro.au

Citation:
Borlace, S., A. Santoso, W. Cai, and M. Collins (2014), Extreme swings of the South Pacific Convergence Zone and the different types of El Niño events, *Geophys. Res. Lett.*, *41*, 4695–4703, doi:10.1002/2014GL060551.

Received 19 MAY 2014
Accepted 26 JUN 2014
Accepted article online 27 JUN 2014
Published online 10 JUL 2014

Extreme swings of the South Pacific Convergence Zone and the different types of El Niño events

Simon Borlace[1,2], Agus Santoso[1,3], Wenju Cai[2], and Matt Collins[4]

[1]ARC Centre of Excellence for Climate System Science, University of New South Wales, Sydney, New South Wales, Australia, [2]CSIRO Marine and Atmospheric Research, Aspendale, Victoria, Australia, [3]Climate Change Research Centre, University of New South Wales, Sydney, New South Wales, Australia, [4]College of Engineering Mathematics and Physical Sciences, University of Exeter, Exeter, UK

Abstract There have been three extreme equatorward swings of the South Pacific Convergence Zone (SPCZ) during the satellite era. These zonal SPCZ (zSPCZ) events coincided with an El Niño of different magnitude and spatial pattern, in which strong anomalous warming reduced the off-equatorial-to-equatorial meridional sea surface temperature (SST) gradient near the dateline, enabling convection to shift equatorward. It is not known, given the short observational record, how and whether different types of El Niño are associated with zSPCZ events. Using perturbed physics ensembles experiments in which SST biases are reduced, we find that zSPCZ events are concurrent with notable eastern Pacific (EP) warming. Central Pacific warming alone is rarely able to produce a swing, even as the climate warms under a CO_2 increase scenario. Only El Niño events with strong EP warming can shift the convective zone. Such co-occurring events are found to increase in frequency under greenhouse warming.

1. Introduction

The location of the South Pacific Convergence Zone (SPCZ), a rainfall band extending southeastward from the Western Pacific Warm Pool to French Polynesia, has been shown to vary on interannual timescales with the El Niño–Southern Oscillation [*Vincent et al.*, 2011; *Brown et al.*, 2012; *Cai et al.*, 2012]. There have been three events (1982/1983, 1991/1992, and 1997/1998) in which the SPCZ underwent an extreme swing equatorward [*Vincent et al.*, 2011]. During these extreme events, referred to here as zonal SPCZ (zSPCZ) events, hydroclimatic conditions are radically altered in the tropical Pacific causing severe environmental and socioeconomic disruption to Pacific island communities. The extreme swing of the SPCZ has been attributed to anomalous warming in the equatorial Pacific Ocean associated with an El Niño, through a reduction in off-equatorial-minus-equatorial meridional sea surface temperature (SST) gradient that extends southeastward from near the dateline [*Cai et al.*, 2012].

El Niño events are projected to undergo significant changes in response to greenhouse warming [*Yeh et al.*, 2009; *Power et al.*, 2013; *Santoso et al.*, 2013], including more frequent occurrences of extreme El Niño and their associated impacts [*Cai et al.*, 2014]. The frequency of zSPCZ events is also projected to increase [*Cai et al.*, 2012]. Yet the link between zSPCZ and El Niño is not fully understood. In particular, it is not currently known whether and how zSPCZ events are related to different types of El Niño events through their differing warming patterns across the equatorial Pacific [*Latif et al.*, 1997].

While El Niño evolution involves a spectrum of spatial patterns, anomalous warming during El Niño events tend to peak either in the equatorial eastern Pacific (EP) toward the South American coast or in the central Pacific (CP) near the dateline [e.g., *Takahashi et al.*, 2011; *Dommenget et al.*, 2013; *Taschetto et al.*, 2014]. Current debate centers on whether the differing locations of maximum anomalous warming represent two dynamically independent phenomena or are part of a continuum [see, e.g., *Fedorov et al.*, 2014]. Regardless of the underlying dynamics, the differing locations of the warming centers have been shown to lead to significant differences in the distribution of surface temperature, rainfall, and wind anomalies in the tropical Pacific [*Kug et al.*, 2009] and beyond [*Larkin and Harrison*, 2005; *Ashok et al.*, 2007; *Wang and Hendon*, 2007; *Weng et al.*, 2007]. If anomalous warming and the associated reduction in the meridional SST gradient about the dateline is what drives an equatorward swing of the SPCZ, then it is expected that the warming pattern associated with either an EP-type (cold tongue El Niño) or a CP-type, also known as the dateline [*Larkin and Harrison*, 2005], Modoki [*Ashok et al.*, 2007], or warm pool [*Kug et al.*, 2009] El Niño could generate a zSPCZ event.

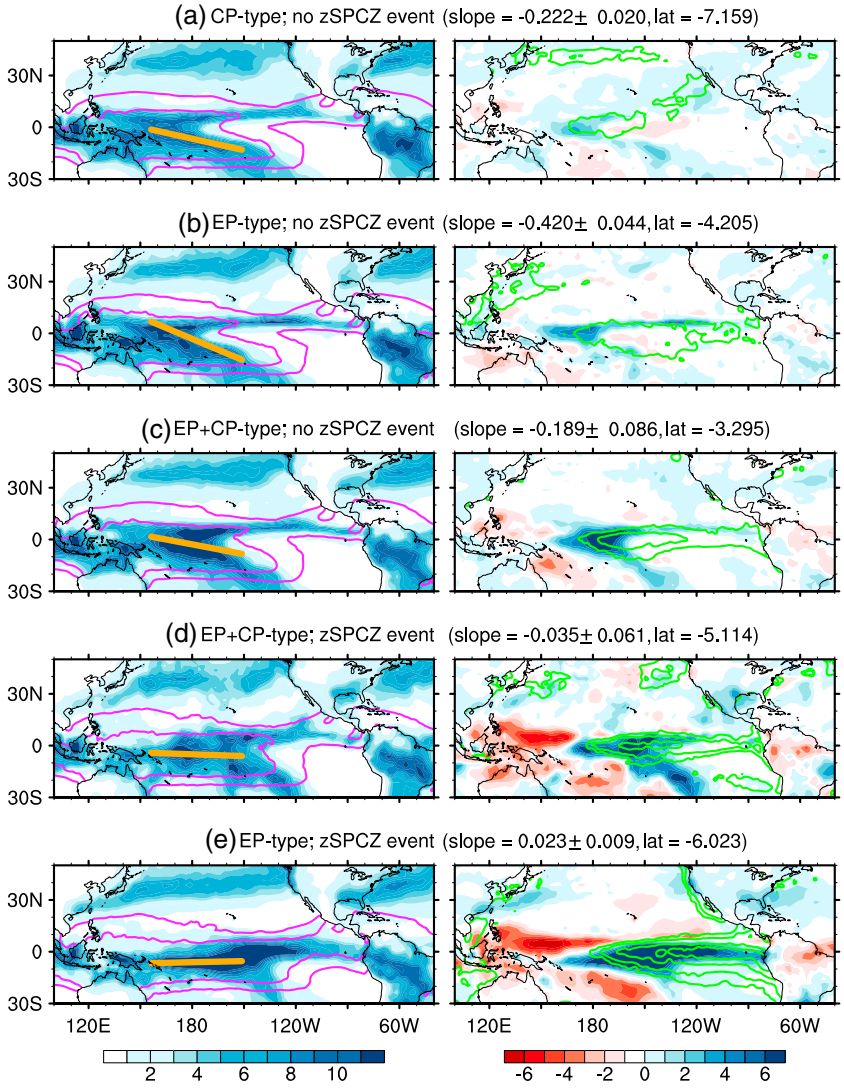

Figure 1. Spatial map of GPCPv2.2 precipitation (left column; shaded contours (mm/day)) and the relative precipitation anomaly (right column; shaded contours (mm/day)). The HadISSTv1.1 26°C and 28°C isotherms (left column; purple contours) are overlayed as well as the 0.5°C, 1°C, 2°C, and 3°C standard deviation SST anomalies (right column; green contours). Each panel shows the multievent mean spatial map for years where there is (a) CP (no zSPCZ) event, (b) EP (no zSPCZ) event, (c) EP + CP (no zSPCZ) event, (d) EP + CP (zSPCZ), and (e) EP (zSPCZ). All anomalies were calculated relative to the period 1979–2008. The slope of the SPCZ is determined from a linear fit to the maximum rainfall at a given longitude between (5°N–25°S, 155°E–140°W) and the mean latitude of the SPCZ within that range.

We have only three zSPCZ events during the satellite era. Two of these clearly co-occurred with EP-type El Niño of the 1982/1983 and 1997/1998. The other, in 1991/1992, co-occurred with an El Niño event that could be classified as a CP type [*Ashok et al.*, 2007; *Yu and Kim*, 2013] (see also Figure 1d). Given such limited number of observed events, examining the link between zSPCZ and El Niño requires the use of climate simulations. In this present study, we utilize observational products and an ensemble of perturbed physics experiments from the HadCM3 coupled global climate model (CGCM) to examine the relationship between the two types of events and zSPCZ and how these interlinks may change under greenhouse warming.

2. Observed Data and Definitions

For observed rainfall we use Global Precipitation Climatology Project version 2.2 data set [*Adler et al.*, 2003] and for SST observations, we use the Hadley Centre Sea Ice and SST data set (HadISST version 1.1) [*Rayner*

et al., 2003]. We focus only on December-January-February (DJF), the peak season for both El Niño warming and the SPCZ rainband position, over 1979–2008. Observed anomalies are calculated relative to the mean climatology over this period.

To date there have been various different methods proposed to differentiate CP-type from EP-type events. [e.g., *Ashok et al*., 2007; *Kao and Yu*, 2009; *Kug et al*., 2009; *Yeh et al*., 2009; *Yu and Kim*, 2010, 2013]. We have chosen to identify a CP-type El Niño using the well-known El Niño Modoki Index (EMI) [*Ashok et al*., 2007] which is defined as $[SSTA]_{central} - 0.5 \times [SSTA]_{east} - 0.5 \times [SSTA]_{west}$ where the brackets indicate the area-averaged sea surface temperature anomaly [SSTA] over central (165°E–140°W, 10°S–10°N), eastern (110°W–70°W, 15°S–5°N), and western (125°E–145°E, 10°S–20°N) Pacific regions. We consider an event a CP type when the EMI is greater than 0.7 standard deviations of interannual variability. For an EP-type El Niño, we use the traditional definition of the Niño3 SST anomaly exceeding 0.5 standard deviations of interannual variability. Under this definition, an event may be classified as a mixture of EP type and CP type (referred to as an EP + CP type) when the anomalous warming in both the equatorial central and eastern Pacific exceeds the specified thresholds.

To verify if the conclusions are insensitive to this choice, we also determine the CP type similar to the approach of *Yeh et al*. [2009], where a CP type occurs if the Niño4 SST anomaly is greater than 0.5 standard deviations and greater than the Niño3 SST anomaly. To be consistent with our earlier approach, as to allow an event to be identified as an EP + CP type, we still employ the criterion of Niño3 SST anomaly greater than 0.5 standard deviations.

Following *Cai et al*. [2012], we identify a zSPCZ event by applying an empirical orthogonal analysis to the rainfall data over the domain (0°–30°S, 160°E–80°W). The first principal pattern captures the northward and southward shift of the SPCZ while the second captures the eastward and westward movement. A zSPCZ event occurs when the first principal component of rainfall is greater than 1 standard deviation and the second is positive [see *Cai et al*., 2012, Figure 1], depicting an equatorward shift of precipitation anomalies east of the dateline. As in *Cai et al*. [2012], the meridional SST gradient is defined here as the average SST over the off-equatorial region (10°S–5°S, 155°E–120°W) minus that over the equatorial region (5°S–0°, 155°E–120°W).

3. Observed SPCZ and Its Link to the Two Types of El Niño

Figure 1 displays the observed rainfall and rainfall anomalies for independent EP and CP event and EP + CP events that occur with and without zSPCZ events. During El Niño events that do not co-occur with a zSPCZ event (Figures 1a–1c), the longitudinal extent of the warm pool is limited to the western Pacific along the equator. The SST anomaly in the central eastern Pacific Ocean is either absent or too weak to significantly reduce the off-equatorial meridional SST gradient near the dateline (see also Figures 2a (purple markers), 2b (green markers), and 2c (light blue markers)). Consequently, the meridional gradient remains strong, preventing an equatorward swing of the rainfall band, and as such, the SPCZ still extends southeastward into the subtropics. Altogether there have been two EP, four CP, and three EP + CP events observed that have not coincided with a zSPCZ event.

The anomalous SST pattern during the 1991/1992 zSPCZ event satisfies both the Niño3 and EMI condition (Figures 1d and 2b; orange marker). The warm pool extends east to approximately 140°W along the equator, and the maximum anomalous warming centered in the central Pacific Ocean is approximately 2 standard deviations. This strong warming largely reduces the meridional SST gradient (also see Figure 2d; orange marker) and, as such, the SPCZ shifts equatorward. The SPCZ no longer extends into the subtropics but assumes a zonally orientated structure, which is objectively quantified by the rainfall band slope of −0.035°lat (latitude)/°lon (longitude), much more confined to the equatorial region than that during non-zSPCZ events (an average of −0.277°lat/°lon).

Despite the dramatic shift in the rainfall band during 1991/1992, this event does not coincide with an extreme El Niño [*Cai et al*., 2014]. During the 1982/1983 and 1997/1998 zSPCZ events on the other hand, the warm pool can be described as extending across the entire equatorial Pacific (Figure 1e), and the core of the positive SST anomaly reaches farther east than that during the 1991/1992 event. The 1982/1983 and 1997/1998 events do not satisfy the EMI condition but do satisfy the rainfall condition for an extreme El Niño (i.e., Niño3 rainfall > 5 mm/d) [*Cai et al*., 2014] and therefore are categorized as extreme EP type (Figure 2b; red markers). In the face of this classification, there is still strong anomalous warming (up to 2 standard

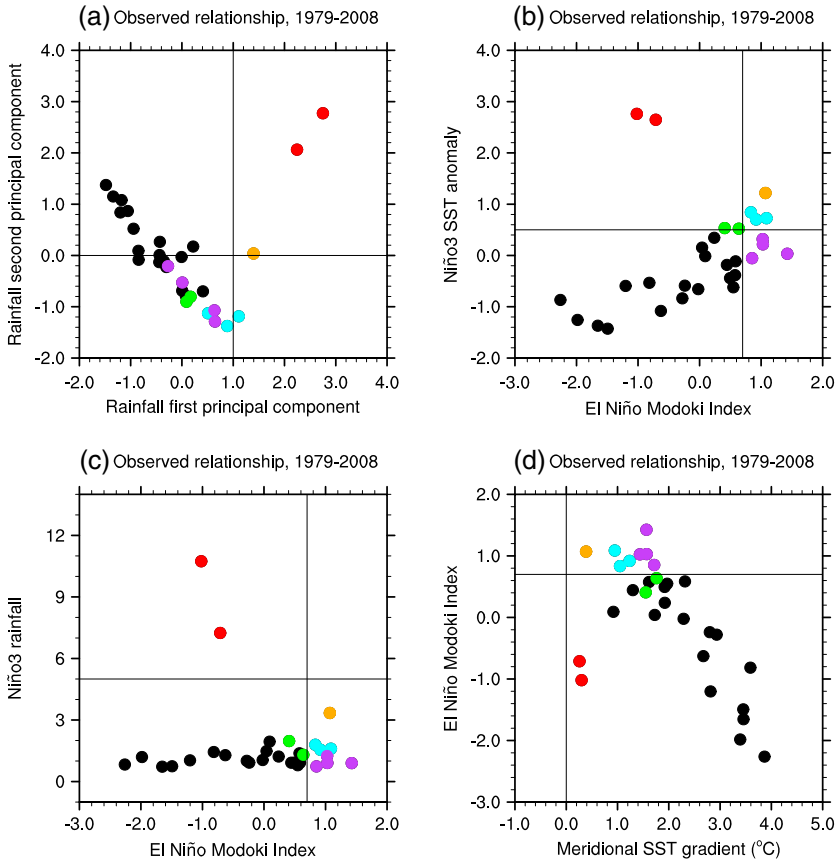

Figure 2. Nonlinear relationship between the first and second rainfall principal component time series. The red markers correspond to EP/no CP/(zSPCZ) events (1982/1983, 1997/1998). The orange markers correspond to EP + CP (zSPCZ) events (1991/1992). The purple markers correspond to CP (no zSPCZ) events (1979/1980, 1990/1991, 1992/1993, and 2004/2005). The light blue markers correspond to EP + CP (no SPCZ) events (1986/1987, 1994/1995, and 2002/2003). The green markers correspond to EP (no zSPCZ) events (1987/1988 and 2006/2007). (b) The relationship between the EMI and Niño3 SST anomaly (°C) time series. (c) The relationship between the EMI and Niño3 rainfall (mm/day) time series. (d) The relationship between the meridional SST gradient and EMI time series.

deviations) just east of the dateline, reducing the meridional SST gradient. The zonal orientation is again depicted by the weak rainfall band slope of 0.023°lat/°lon, with strongly positive first and second rainfall principal components (Figure 2a; red markers).

4. Simulated zSPCZ Events and the Link to El Niño Under Greenhouse Warming

Understanding El Niño–Southern Oscillation variability and impacts is difficult due to the limited observational record [*Vecchi and Wittenberg*, 2010]. Although CGCMs serve as an important tool, intrinsic model biases and the differing physical parameterizations across models are confounding factors when trying to assess regional changes in climate such as those studied here. An ensemble approach using a collection of different climate models, such as that facilitated through the Coupled Model Intercomparison Project, can provide some measure of such uncertainty [*Collins et al.*, 2011]. Another approach is the perturbed physics ensemble in which uncertain physical parameters are varied within a single model structure. The advantage of the perturbed physics ensembles is that they allow a more systematic approach for investigating simulated processes and feedbacks. Furthermore, the ensemble used here employs flux adjustments that alleviate problems with biases in SSTs that are common to all models.

We focus on a set of 17 perturbed physics ensemble (PPE) HadCM3 CGCM experiments with fixed CO_2 (control) and climate change experiments forced with a 1% yr^{-1} CO_2 increase [*Collins et al.*, 2011]. Known SST

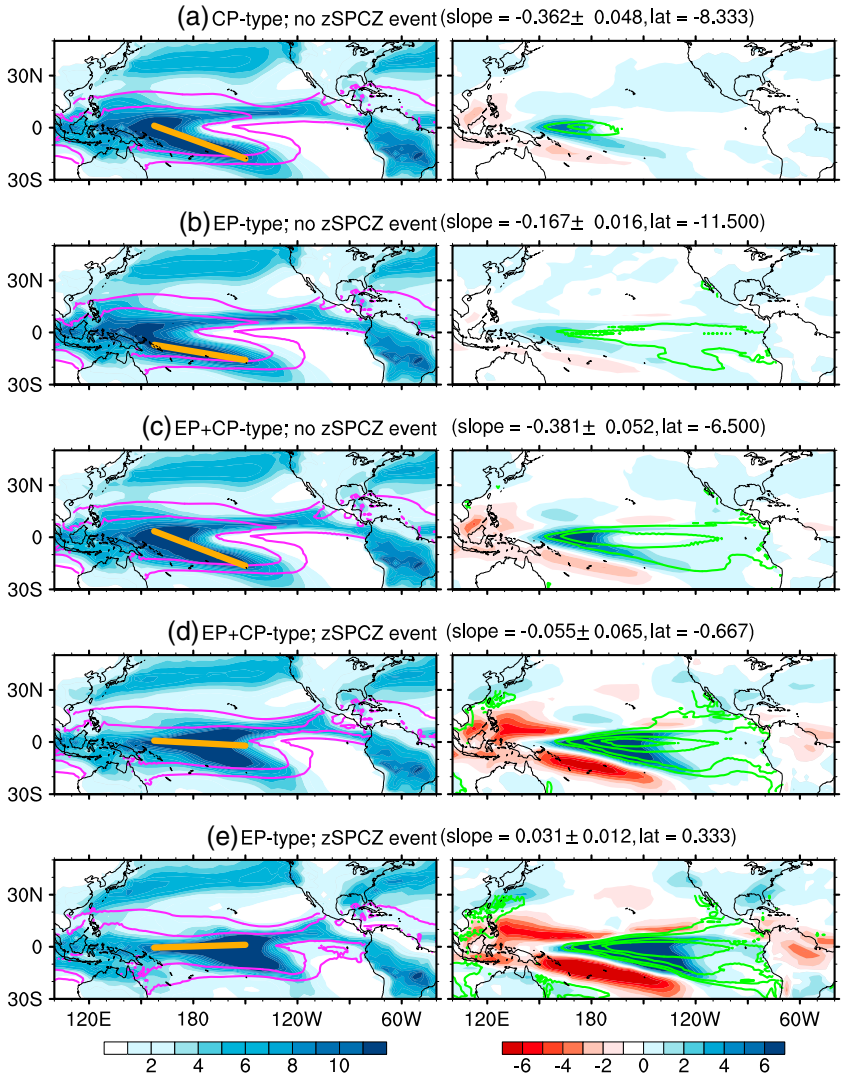

Figure 3. Multievent ensemble spatial map of HadCM3 precipitation (left column; shaded contours (mm/day)) and the relative precipitation anomaly (right column; shaded contours (mm/day)) for the simulated control period (1891–1990). The simulated 26°C and 28°C isotherms (left column; purple contours) are overlayed as well as the 0.5°C, 1°C, 2°C, and 3°C standard deviation detrended SST anomalies (right column; green contours). Each panel shows the multievent mean spatial map for years where there is (a) CP (no zSPCZ) event, (b) EP (no zSPCZ) event, (c) EP + CP (no zSPCZ) event, (d) EP + CP (zSPCZ), and (e) EP (zSPCZ). The slope of the SPCZ is determined from a linear fit to the maximum rainfall at a given longitude between (5°N–25°S, 155°E–140°W) and the mean latitude of the SPCZ within that range.

biases in the model are considerably reduced through a fixed, seasonally varying flux adjustment. We identify a subset of the ensemble runs for analysis based on the criteria that (1) the run is able to simulate zonal swings of the SPCZ (i.e., nonlinear relationship between the first and second rainfall principal component) and (2) the run is able to simulate a minimum of one EP, one EP + CP, and one CP with at least one of any of these coinciding with a zSPCZ event. In total, 13 of 17 runs satisfy these criterions.

The ensemble runs show that zSPCZ events co-occur with EP + CP El Niño (52 events) more frequently than EP El Niño (nine events) in the control period. This is in contrast to the limited observations in which zSPCZ events co-occurred twice with EP El Niño events (1982/1983 and 1997/1998) compared to once with EP + CP El Niño (1991/1992). Similar to observations, however, virtually none of the zSPCZ events co-occur with CP-type El Niño.

As with the observations (Figure 1), the simulated El Niño events that do not coincide with a zSPCZ event have a warm pool that is largely confined to the west and are associated with very limited anomalous SST warming in the central eastern Pacific Ocean (Figures 3a–3c). In contrast, and again consistent with

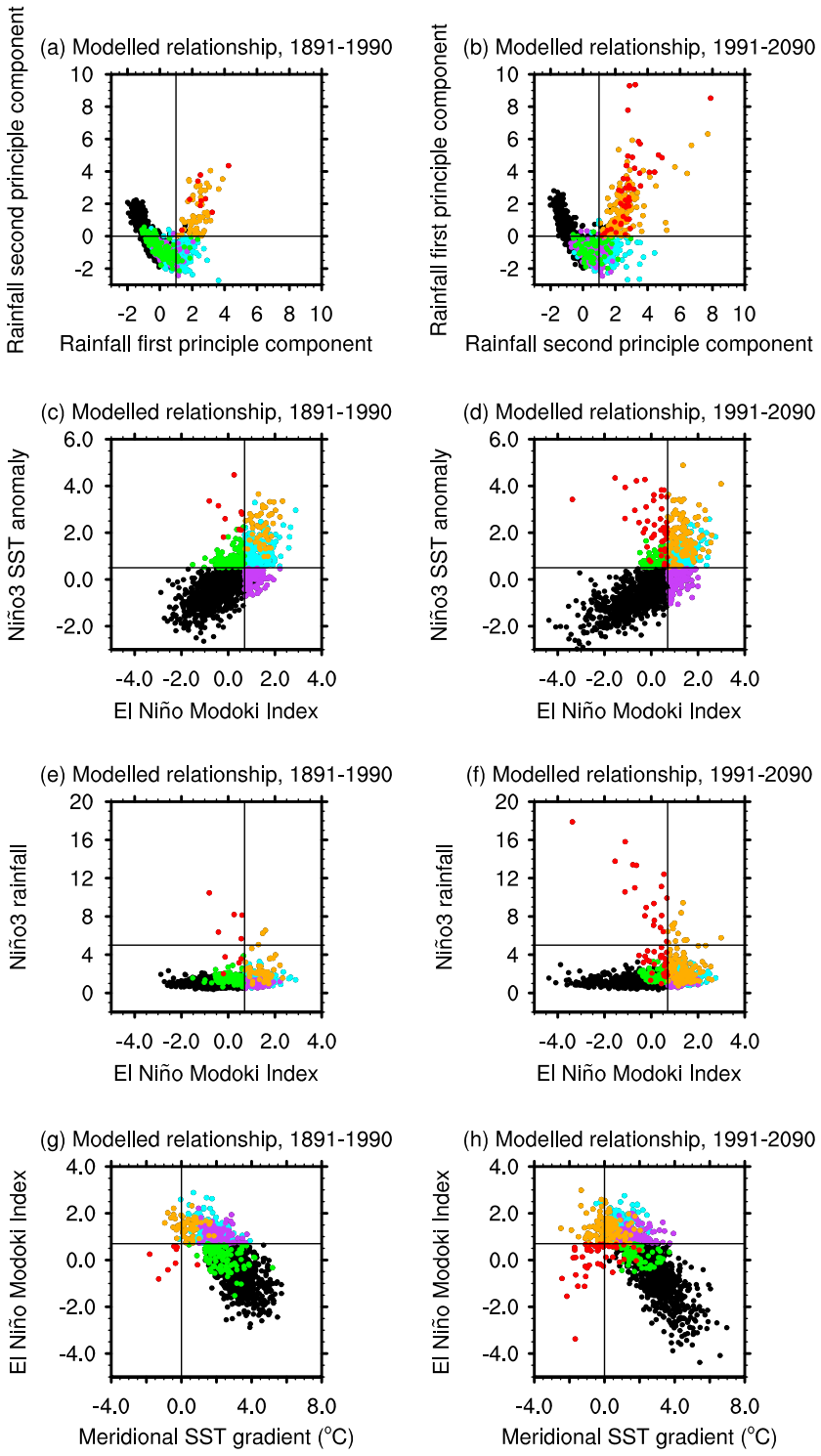

Figure 4. Nonlinear relationship between the first and second rainfall principal component time series (a) for control period (1891–1990) and (b) for the climate change period (1991–2090). The red markers correspond to EP/no CP/ (zSPCZ) events. The orange markers correspond to EP + CP (zSPCZ) events. The purple markers correspond to CP (no zSPCZ) events. The light blue markers correspond to EP + CP (no SPCZ) events. The green markers correspond to EP (no zSPCZ) events. The relationship between the EMI and Niño3 SST anomaly (°C) time series (c) for the control change period and (d) for the climate change period. The relationship between the EMI and Niño3 rainfall (mm/day) time series (e) for the control change period and (f) for the climate change period. The relationship between the meridional SST gradient and EMI time series (g) for the control change period and (h) for the climate change period.

observations, the EP + CP- and EP-type El Niño events that do coincide with zSPCZ events have a warm pool that extends east of 140°W, in association with a strong SST anomaly in the central eastern part of the basin. This leads to a reduction in the meridional SST gradient (Figure 4g), thus allowing for the SPCZ rainfall band to align zonally along the equator. An extreme El Niño is not required to simulate a zSPCZ event (Figure 4e).

Under greenhouse warming, the HadCM3 CGCM simulates 181% increase in frequency of zSPCZ events, that is, by almost a factor of 3, from a multirun total of 62 events in the control period to 174 in the climate change period. The interrun consensus is strong with 12 of the 13 runs showing an increase in the future climate (Table S1 in the supporting information). This future increase is comparable to that found by *Cai et al*. [2012], who found a 214% increase across 12 perturbed physics experiments of the HadCM3 model, with all 12 showing an increase in the future climate.

The future increase in zSPCZ events corresponds with an increase in co-occurrences with EP- and EP + CP-type events, without any of the two types of event being a clear dominating factor (Figures 4c and 4d). This is despite there being no significant change in the total number of El Niño events in a warming climate (Tables S1 and S2). Using the event identification approach of *Yeh et al*. [2009], the statistics do change, since the Yeh et al. approach classifies several of the EMI-based EP + CP events into EP-type events (Tables S3 and S4). However, this does not change the main result in that zSPCZ occurrences with both EP and EP + CP type of El Niño events increase substantially under greenhouse warming.

Using either event definition, the model simulates only one CP-type El Niño event that co-occurs with a zSPCZ event during the control period (see Table S1). Under climate change, although this increases to four events (EMI based) or six events (Yeh et al. approach), these are still a small number over the aggregated 1300 years.

5. Discussion and Conclusions

Our analysis of observational data and PPE demonstrates that zSPCZ events co-occur with El Niño events of either an EP type or a mixed EP and CP type (EP + CP). No zSPCZ has ever co-occurred with a CP El Niño in observations, and virtually none in the 1300 years of aggregated model runs in the fixed-CO_2 control period (1891–1990). This finding is robust regardless of the choice of methods used to distinguish the different types of El Niño. This stems from the fact that EP- and EP + CP-type El Niño events tend to involve stronger anomalous warming that peaks during the boreal winter, in excess of 1°C in both central and eastern equatorial Pacific, than CP El Niño (Figures S1 and S2). Strong anomalous warming is required to reduce the off-equatorial meridional SST gradient to a near-zero value for inducing an equatorward swing of the SPCZ.

At present there is still much debate as to whether the CP and EP El Niño really represent two independent phenomena or are simply part of a continuum [see, e.g., *Fedorov et al*., 2014]. This latter view reflects the challenge in distinguishing the dynamics of one type from the other. It is in this light that our present study has chosen to accommodate the mixed EP + CP type in terms of the spatial pattern of the SST anomalies. By using a more restrictive definition of EP-type warm events according to that of *Yeh et al*. [2009] (i.e., Niño3 SST anomaly $>$ 0.5 standard deviation and Niño3 SST anomaly $>$ Niño4 SST anomaly), El Niño events are allowed to be classified as either a CP or an EP type. In this case, there are years in which zSPCZ events co-occur with a CP-type or Modoki El Niño (see Table S3), as all of the EP + CP El Niño events are now classified as CP-type events. This approach though would overlook the importance of eastern Pacific warming—a feature that is highlighted in this present study.

In addition, considering the persistence of an anomalous warming pattern in the central Pacific from boreal summer [see *Ashok et al*., 2007] would classify the EP + CP-type events that have stronger persistence as a Modoki (Figure S3). Those in which the warming does not onset until boreal spring would be classified as canonical El Niño. With this consideration, the four EP + CP observed events (1986/1987, 1991/1992, 1994/1995, 2002/2003) would be classified as Modoki events, still with only the 1991/1992 event that co-occurred with a zSPCZ event. The model experiments, however, show significant variability in the evolution of the maximum anomalous warming associated with EP + CP-type El Niño (Figure S4). Such variety of El Niño behavior and characteristics may be feasible in the real system, for instance through multidecadal variability, not constrained by the currently limited observational record [e.g., *Wittenberg*, 2009; *Borlace et al*., 2013]. To account for this possibility, and because the zonal SPCZ is most developed in DJF, the notion of an EP + CP-type event defined for the DJF season appears reasonable. Nonetheless, this present study does

not aim to argue for the dependence or independence between CP and EP events, but to highlight the role of the eastern Pacific warm anomaly in the occurrences of zonal SPCZ events.

Understanding the physical mechanisms that limit the growth of CP-type SST anomalies (i.e., local air-sea response, thermocline feedbacks, zonal advection, extratropical forcing, and meridional modes of variability) is also still under investigation [*Yeh et al*., 2014; *Fedorov et al*., 2014]. It has also been suggested that the maximum anomalous warming associated with CP-type El Niño tends to peak closer to November-December [*Ashok et al*., 2007; *Kug et al*., 2009] which means the strongest warming may occur near the dateline slightly before the SPCZ has started to develop. As such, the anomalous warming may be weakening over the course of the boreal winter and is never strong enough to induce an extreme swing. This phase lag may also explain why CP type and zSPCZ never co-occur, not even in a warming climate.

Our analysis thus demonstrates that zonal SPCZ extreme events involve strong eastern tropical Pacific warming, which can extend toward the central tropical Pacific (EP + CP type). Occurrences of strong anomalous warming in the usually cold and dry eastern equatorial Pacific region tend to shift the Western Pacific Warm Pool eastward, drawing moisture, rainfall, and convection toward the coast of South America. Such changes depict more severe disruption to the ocean and atmosphere circulation of the tropical Pacific. The associated processes involve strong nonlinearity in the Niño3 region, as reflected by positive skewness in SST in which warm SST anomalies tend to grow stronger in amplitude than cold anomalies—as opposed to weak negative skewness in the central Pacific [*Burgers and Stephenson*, 1999]. Under greenhouse warming, the eastern equatorial Pacific warms faster than in the west in models [*Xie et al*., 2010; *Tokinaga et al*., 2012], allowing weaker positive SST anomalies to generate the same degree of magnitude in atmospheric response seen in the control period [*Cai et al*., 2014]. As such, under global warming, zonal SPCZ extreme events tend to co-occur more frequently with El Niño events. Increased frequency in such co-occurrences highlights the severity of global warming impact.

Acknowledgments

The Global Precipitation Climatology Project version 2.2 data set was obtained online from the Earth System Research Laboratory (http://www.ersl.noaa.gov/psd/data/gridded/data.gpcp.html; data set name: precip.mon.mean.nc). Hadley Centre Sea Ice and SST Temperature data set version 1.1 can be obtained from the Met Office Hadley Centre (http://www.metoffice.gov.uk/hadobs/hadisst/; data set name: HadISST_sst_nc.gz). The perturbed physics ensemble (PPE) HadCM3 CGCM experiments are available online from the Centre for Environmental Data Archival (http://badc.nerc.ac.uk/view/badc.nerc.ac.uk__ATOM__dataent_12024019658225569). This research was funded, in part, by the Australian Climate Change Science Programme, and, in part, by the ARC Centre of Excellence for Climate System Science (grant CE110001028). A.S. is supported by the Australian Research Council. M.C. was supported by NE/I022841/1. We would also like to thank two anonymous reviewers for their insightful comments that helped improve the present manuscript.

The Editor thanks two anonymous reviewers for their assistance in evaluating this paper.

References

Adler, R. F., et al. (2003), The Version 2 Global Precipitation Climatology Project (GPCP) monthly precipitation analysis (1979–present), *J. Hydrometeorol.*, *4*, 1147–1167.

Ashok, K., S. K. Behera, S. A. Rao, H. Weng, and T. Yamagata (2007), El Niño Modoki and its possible teleconnection, *J. Geophys. Res.*, *112*, C11007, doi:10.1029/2006JC003798.

Borlace, S., W. Cai, and A. Santoso (2013), Multidecadal ENSO amplitude variability in a 1000-year simulation of a Coupled Global Climate Model: Implications for observed ENSO variability, *J. Clim.*, *26*, 9399–9407, doi:10.1175/JCLI-D-13-00281.1.

Brown, J. R., A. F. Moise, and F. P. Delange (2012), Change in the South Pacific Convergence Zone in the IPCC AR4 future climate projections, *Clim. Dyn.*, *39*, 1–19.

Burgers, G., and D. B. Stephenson (1999), The "normality" of El Niño, *Geophys. Res. Lett.*, *26*, 1027–1030, doi:10.1029/1999GL900161.

Cai, W., et al. (2012), More extreme swings of the South Pacific Convergence Zone due to greenhouse warming, *Nature*, *488*, 365–369, doi:10.1038/nature11358.

Cai, W., et al. (2014), Increase frequency of extreme El Niño events due to greenhouse warming, *Nat. Clim. Change*, *4*, 111–116, doi:10.1038/nclimate2100.

Collins, M., B. B. B. Booth, B. Bhaskaran, G. R. Harris, J. M. Murphy, D. M. H. Sexton, and M. J. Webb (2011), Climate model errors, feedbacks and forcings: A comparison of perturbed physics and multi-model ensembles, *Clim. Dyn.*, *36*, 1737–1766, doi:10.1007/s00382-010-0808-0.

Dommenget, D., T. Bayr, and C. Frauen (2013), Analysis of the non-linearity in the pattern and time evolution of El Niño Southern Oscillation, *Clim. Dyn.*, *40*, 2825–2847, doi:10.1007/s00382-012-1475-0.

Fedorov, A. V., S. Hu, M. Lengaigne, and E. Guilyardi (2014), The impact of westerly wind bursts and ocean initial state on the development, and diversity of El Niño events, *Clim. Dyn.*, doi:10.1007/s00382-014-2126-4.

Kao, H., and J.-Y. Yu (2009), Contrasting eastern-Pacific and central Pacific types of ENSO, *J. Clim.*, *22*, 615–632, doi:10.1175/2008JCLI2309.1.

Kug, J.-S., F.-F. Jin, and S.-I. An (2009), Two types of El Niño events: Cold tongue El Niño and warm pool El Niño, *J. Clim.*, *22*, 1499–1515, doi:10.1175/2008JCLI2624.1.

Larkin, N. K., and D. E. Harrison (2005), Global seasonal temperature and precipitation anomalies during El Niño autumn and winter, *Geophys. Res. Lett.*, *32*, L16705, doi:10.1029/2005GL022860.

Latif, M., R. Kleeman, and C. Eckert (1997), Greenhouse warming, decadal variability, or El Niño? An attempt to understand the anomalous 1990s, *J. Clim.*, *10*, 2221–2239, doi:10.1175/1520-0442(1997)010<2221:GWDVOE>2.0.CO;2.

Power, S., F. Delage, C. Chung, G. Kociuba, and K. Keay (2013), Robust twenty-first century projections of El Niño and related precipitation variability, *Nature*, *502*, 541–545, doi:10.1038/nature12580.

Rayner, N. A., D. E. Parker, E. B. Horton, C. K. Folland, L. V. Alexander, D. P. Rowell, E. C. Kent, and A. Kaplan (2003), Global analyses of sea surface temperature, sea ice, and night marine temperature since the late nineteenth century, *J. Geophys. Res.*, *108*(D14), 4407, doi:10.1029/2002JD002670.

Santoso, A., S. McGregor, F.-F. Jin, W. Cai, M. H. England, S.-I. An, M. J. McPhaden, and E. Guilyardi (2013), Late-twentieth-century emergence of the El Niño propagation asymmetry and future projections, *Nature*, *504*, 126–130, doi:10.1038/nature12683.

Takahashi, K., A. Montecinos, K. Goubanova, and B. Dewitte (2011), ENSO regimes: Reinterpreting the canonical and Modoki El Niño, *Geophys. Res. Lett.*, *38*, L10704, doi:10.1029/2011GL047364.

Taschetto, A. S., A. Sen Gupta, N. C. Jourdain, A. Santoso, C. C. Ummenhofer, and M. H. England (2014), Cold tongue and warm pool ENSO events in CMIP5: Mean state and future projections, *J. Clim.*, *27*, 2861–2885, doi:10.1175/JCLI-D-13-00437.1.

Tokinaga, H., S.-P. Xie, C. Deser, Y. Kosaka, and Y. M. Okumura (2012), Slowdown of the Walker circulation driven by tropical Indo-Pacific warming, *Nature*, *491*, 439–443.

Vecchi, G. A., and A. Wittenberg (2010), El Niño and our future climate: Where do we stand?, *Wiley Interdiscip. Rev.: Clim. Change*, *1*, 260–270, doi:10.1002/wcc.33.

Vincent, E. M., M. Lengaigne, C. E. Menkes, N. C. Jourdain, P. Marchesiello, and G. Madec (2011), Interannual variability of the South Pacific Convergence Zone and implications for tropical cyclone genesis, *Clim. Dyn.*, *36*, 1881–1896.

Wang, G., and H. H. Hendon (2007), Sensitivity of Australian rainfall to inter-El Niño variations, *J. Clim.*, *20*, 4211–4226, doi:10.1175/JCLI4228.1.

Weng, H., K. Ashok, S. K. Behera, S. A. Rao, and T. Yamagata (2007), Impacts of recent El Niño Modoki on dry/wet conditions in the Pacific rim during boreal summer, *Clim. Dyn.*, *29*, 113–129, doi:10.1007/s00382-007-0234-0.

Wittenberg, A. T. (2009), Are historical records sufficient to constrain ENSO simulations?, *Geophys. Res. Lett.*, *36*, L12702, doi:10.1029/2009GL038710.

Xie, S.-P., C. Deser, G. A. Vecchi, J. Ma, H. Teng, and A. Wittenberg (2010), Global warming pattern formation: Sea surface temperature and rainfall, *J. Clim.*, *23*, 966–986, doi:10.1175/2009JCLI3329.1.

Yeh, S.-W., J.-S. Kug, B. DeWitte, M.-H. Kwon, B. Kirtman, and F.-F. Jin (2009), El Niño in a changing climate, *Nature*, *461*, 511–514, doi:10.1038/nature08316.

Yeh, S.-W., J.-S. Kug, and S.-I. An (2014), Recent progress on two types of El Niño: Observations, dynamics and future changes, *Asia-Pac. J. Atmos. Sci*, *50*, 69–81, doi:10.1007/s13143-014-0028-3.

Yu, J.-Y., and S. T. Kim (2010), Three evolution patterns of central Pacific El Niño, *Geophys. Res. Lett.*, *37*, L08706, doi:10.1029/2010GL042810.

Yu, J.-Y., and S. T. Kim (2013), Identifying the types of major El Niño events since 1870, *Int. J. Climatol.*, *33*, 2105–2112, doi:10.1002/joc.3575.